IOP PUBLISHING EUROPEAN JOURNAL OF PHYSICS

Eur. J. Phys. **28** (2007) 1007–1020 doi:10.1088/0143-0807/28/5/023

Experiments with a magnetically controlled pendulum

Yaakov Kraftmakher

Department of Physics, Bar-Ilan University, Ramat-Gan 52900, Israel

E-mail: krafty@mail.biu.ac.il

Received 17 April 2007, in final form 13 June 2007
Published 8 August 2007
Online at stacks.iop.org/EJP/28/1007

Abstract

A magnetically controlled pendulum is used for observing free and forced oscillations, including nonlinear oscillations and chaotic motion. A data-acquisition system stores the data and displays time series of the oscillations and related phase plane plots, Poincaré maps, Fourier spectra and histograms. The decay constant of the pendulum can be modified by positive or negative feedback. The apparatus, except for the data-acquisition system, is extremely simple and low cost, and can be assembled in a short time. The wide possibilities of varying the parameters of the pendulum make the experiments suitable for student projects.

1. Introduction

Many papers have been published during recent decades on nonlinear oscillations and chaotic motion, and only a small selection of them are mentioned here. Schmidt and Childers (1984) described a magnetic pendulum for demonstrations of phase transitions. Dixon *et al* (1985) studied amplitude jumps of a nonlinear pendulum, including the motion during a jump. Grosu and Ursu (1986) described a setup for teaching linear and nonlinear oscillations, including bent tuning curves. Marega *et al* (1990) presented an electromechanical analogue for Landau's theory of phase transitions. Krautz (1993) developed a classroom demonstration based on computer animation of a driven pendulum. Siahmakoun *et al* (1997) investigated the dynamics of a sinusoidally driven pendulum in a repulsive magnetic field. Regions of periodic and chaotic behaviour, amplitude jumps, hysteresis and bistable states were observed. Blackburn and Baker (1998) compared commercially available chaotic pendulums. Berdahl and Vander Lugt (2001) reported on a magnetically driven chaotic pendulum. DeSerio (2003) studied nonlinear dynamics with a commercial chaotic pendulum. The pendulum was modified to determine Poincaré sections, fractal dimensions and Lyapunov exponents. Two hundred Poincaré sections were obtained during one run, and the role of the decay constant of the pendulum was shown. Laws (2004) described several experiments on linear and nonlinear

oscillations, including chaotic motion. Baker (2006) considered the application of probability concepts to deterministic systems. The probability distribution of angular displacement of a pendulum was obtained for nonlinear and chaotic motion.

Nonlinear dynamics and chaos are considered in many textbooks (e.g., Moon (1987), Baker and Gollub (1996), José and Saletan (1998)). Seemingly, the apparatus for teaching this subject should provide the following options:

- varying the amplitude and frequency of the driving force or torque;
- displaying time series of the oscillations, phase plane plots, Poincaré maps, and Fourier spectra and histograms of position and velocity;
- varying the natural frequency and the strength of nonlinearity of the oscillator;
- changing the decay constant of the oscillator, preferably with no changes in its natural frequency;
- using low-cost components, preferably of equipment commonly available in student laboratories.

2. Apparatus

For the experiments described below, we use a low-cost and easy-to-build magnetically controlled pendulum suitable for studying nonlinear oscillations and chaotic motion. The *ScienceWorkshop* data-acquisition system with *DataStudio* software from PASCO scientific controls the experiments.

2.1. The pendulum

A magnetically controlled pendulum represents a well-known device. Several modifications of such a pendulum have already been described (Schmidt and Childers (1984), Marega *et al* (1990), Siahmakoun *et al* (1997), Berdahl and Vander Lugt (2001), Kraftmakher (2005), (2007a)). External magnetic fields may serve for driving the pendulum and/or for modifying the restoring torque.

In our pendulum (figure 1), two similar permanent magnets are positioned on a thin aluminium rod, with a pivot attached to the axle of the PASCO's *Rotary motion sensor* (CI-6538). Both magnets are strong ceramic magnets, $12 \times 12 \times 12$ mm^3 in size, magnetized to about 1.2 T (Kraftmakher (2007b)). The upper magnet is positioned 25 mm above the pivot, and the lower 75 mm below. The axis of the upper magnetic dipole is aligned horizontally. The lower magnet can be aligned horizontally (pendulum with feedback) or vertically (other experiments). The magnets are tightly put in plastic chutes, which makes easy to change their orientation.

An 800-turn coil (PASCO, SF-8611) with a magnetic core is positioned above the upper magnet. The interaction of its magnetic field with the magnet drives the pendulum. A 320-turn coil, about 14 cm in diameter, can be positioned beneath the pendulum and fed by a dc supply. The magnetic field of this coil provides attractive or repulsive action on the lower magnet aligned vertically and thus modifies the restoring torque and its angular dependence.

An aluminium disc is attached to the other end of the axle of the *Rotary motion sensor* and subjected to the magnetic field of another permanent magnet (not shown in figure 1). The position of this magnet controls the decay constant of the pendulum. It is worth remembering that the driving coil connected to a source of low output resistance also provides damping action on a moving magnet. Therefore, the coil should be removed or disconnected when observing free oscillations of the pendulum. On the other hand, a study of the damping action of a coil loaded by different resistors would be an additional topic illustrating Lenz's law.

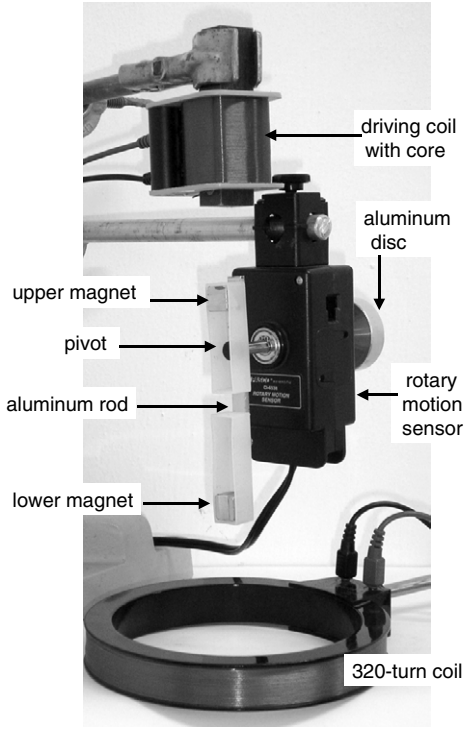

Figure 1. The magnetically controlled pendulum.

In addition, it is possible to tilt the pendulum and thus to decrease the restoring torque due to gravity (the so-called variable g pendulum).

2.2. The experiments

The restoring and driving torques can be made strongly dependent on the angular position of the pendulum. The nonlinearity of the driving torque strongly depends on the gap between the magnetic core of the driving coil and the upper magnet, while the nonlinearity of the restoring torque is controllable by the dc magnetic field produced by the 320-turn coil. The two actions can be applied independently. In the experiments presented, only one source of nonlinearity is chosen, while combining of the two actions is open for further experimentation.

The motion equation for the pendulum can be presented only in a very general form reflecting the two nonlinearities:

$$\theta'' + \gamma\theta' + \omega_0^2(\theta)\theta = F(\theta)\sin\omega t, \tag{1}$$

where θ is the angular position of the pendulum, $\gamma\theta'$ is the damping term, $\omega_0^2(\theta)$ is the natural frequency, and $F(\theta)$ is a function of the angular position. The angular dependence of the natural frequency can be modified by changing the dc current in the 320-turn coil and the distance between the coil and the lower magnet. The coefficient γ can be taken constant only when the pendulum is magnetically damped. This point was considered by Squire (1986).

The nonlinear properties of the pendulum thus strongly depend on its real arrangement, and additional efforts are needed for specifying the motion equation for different setups. A

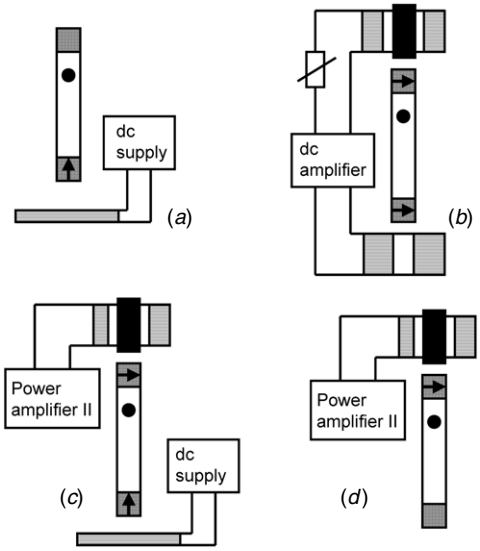

Figure 2. General scheme of the experiments: (a) free oscillations; (b) pendulum with feedback; (c) bent tuning curves; (d) nonlinear oscillations and chaotic motion. The arrows indicate the alignment of magnetic dipoles. Magnets shown without arrows can be excluded.

theoretical analysis of the experiments is therefore not so simple, which is a disadvantage of the apparatus.

Experiments with the pendulum presented here include the following items:

- the amplitude dependence of the oscillation period of the pendulum with the additional nonlinearity brought in by an external magnetic field;
- the potential well of the pendulum with the additional nonlinearity;
- the pendulum with positive or negative feedback: dependence of the decay constant on the feedback factor;
- bent tuning curves of the nonlinear pendulum: the hysteresis and amplitude and phase jumps in the vicinity of resonance;
- transient processes after changing the amplitude or frequency of the driving torque and response to a step or an impulse function;
- nonlinear oscillations presented as time series, phase plane plots, Fourier spectra and histograms;
- chaotic motion and Poincaré sections.

The arrangements of the setup used in various experiments are shown in a general scheme (figure 2).

Two preliminary measurements are useful to check the apparatus (figure 3). First, the angular position of the pendulum is determined versus the current in the driving coil under nearly equilibrium conditions. By increasing the gap, the nonlinearity in the driving torque can be highly reduced.

Second, free oscillations of the pendulum are observed with and without magnetic damping. For determining the decay constant, the data should be fitted by an exponentially decaying sinusoid. As an alternative, we use the *User-defined fit* tool provided by *DataStudio*. Simply, a curve $A\exp(-Bt)$ that fits the envelope of the oscillations is added to the graph

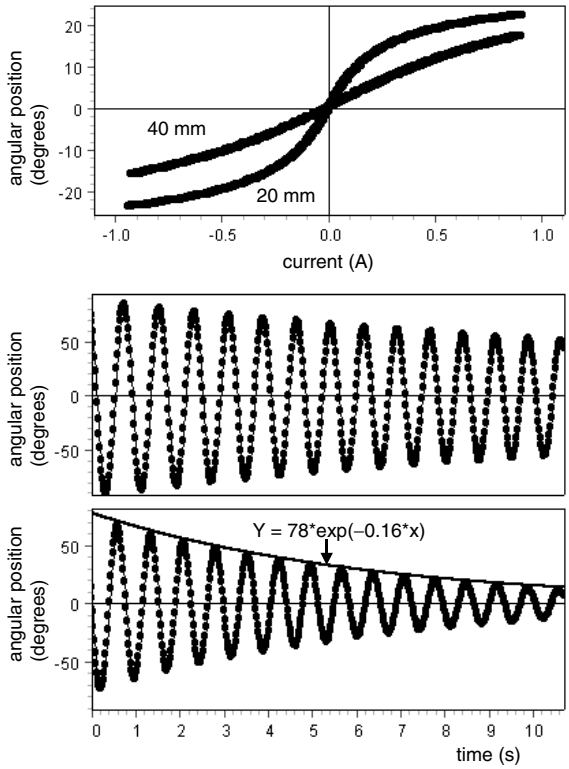

Figure 3. From top to bottom: angular position of the pendulum versus electric current in the driving coil for 20 mm and 40 mm gap between the upper magnet and the magnetic core of the coil; free oscillations without magnetic damping; free oscillations with magnetic damping. The method of determining the decay constant with *DataStudio* is shown.

of free oscillations. The numerical values of A and B are varied for achieving an acceptable fit. The accuracy of this procedure is about 10%. Without magnetic damping, the decay does not obey an exponential law because the dry friction in the *Rotary motion sensor* is not proportional to the angular velocity.

3. Free oscillations

Free oscillations of the pendulum are observed when the restoring torque is modified by a dc magnetic field and when the decay constant of the pendulum is modified by positive or negative feedback.

3.1. The period and potential well of the pendulum

The period of free oscillations of a usual pendulum depends on their amplitude: for amplitudes close to 90°, the period becomes about 17% longer than for small-angle oscillations (e.g., Lewowski and Woźniak (2002)). For our pendulum, this dependence becomes significant even at small oscillation amplitudes. The lower magnet is aligned vertically, and the upper magnet is unnecessary in these measurements (see figure 2(a)). The interaction between

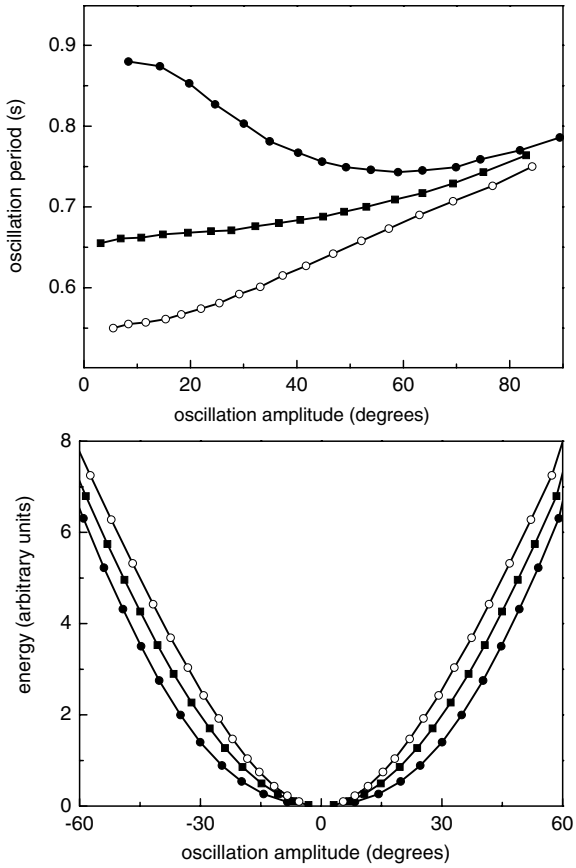

Figure 4. The period of free oscillations versus their amplitude and the potential well of the pendulum: ■—with no current in the coil, ● and ○—two directions of a 0.5 A current.

the lower magnet of the pendulum and the dc magnetic field of the 320-turn coil produces a repulsive or attractive force on the pendulum, in addition to the gravitational force. The additional force significantly modifies the restoring torque and thus the amplitude dependence of the period of free oscillations.

For determining the angular dependence of the oscillation period, the pendulum is displaced by an angle of 90° and released. During the motion, one triggers new measurements for every 2–3 oscillations, and more than ten records are obtainable in one decay period. Then the *Fit/Sine fit* tool of *DataStudio* is used to fit the consecutive data. The tool fits the data by the function

$$Y = A\sin[2\pi(t - C)/B] + D, \tag{2}$$

where A and B are the amplitude and period of the oscillations, D is an offset, and C reflects the initial phase φ of the oscillations: $\varphi = \omega C = 2\pi C/B$.

The fit thus immediately provides the amplitude and the period of the oscillation. The measurements are performed with no current in the coil and with a 0.5 A dc current providing a repulsive or attractive action on the lower magnet. In these measurements, the distance between the centres of the lower magnet and of the coil is 70 mm. The additional nonlinearity is 'soft' or 'hard', depending on the direction of the current in the coil (figure 4). The

difference in the periods reaches a maximum at small-angle oscillations because in this region the attractive or repulsive action of the coil becomes stronger. Clearly, the properties of the pendulum depend on the current in the coil and on its position relative to the lower magnet.

By observations of free oscillations, it is easy to evaluate the potential well of the pendulum (Pippard (1978), DeSerio (2003), Thornton and Marion (2004)). For this purpose, we take data on the amplitude dependence of the oscillation period. For each oscillation, the full energy of the pendulum is proportional to the square of its maximum angular velocity. In our case, the energy is proportional to $(A/B)^2$, where A and B are the quantities in equation (2) evaluated by the *Fit/Sine fit* tool. A graph of the energy versus the oscillation amplitude represents the potential well. As expected, the relative changes in the potential for different strengths of nonlinearity are most significant at small oscillation amplitudes. Rigorously speaking, the pendulum subjected to the repulsive action of the coil has two equilibrium positions on both sides of the vertical. This phenomenon is insignificant in the present measurements because the wells are shallow and positioned very close to the vertical. Therefore, they are not seen in the graph.

The procedure used here for the determination of the potential well assumes a symmetrical shape of the well. This approach is inapplicable when the oscillations are asymmetrical. In such cases, data for the potential well are obtainable from the phase plane plots.

3.2. The pendulum with feedback

This experiment is useful for introducing the concept of feedback, which is very important in physics and modern technologies. To change the decay constant of the pendulum by feedback, both magnets are aligned horizontally (see figure 2(b)). The lower magnet of the pendulum and a 3200-turn coil (PASCO, SF-8613) beneath it serve for producing the feedback voltage. With the axis of the lower magnetic dipole aligned horizontally, the feedback voltage is of the same frequency as the oscillations of the pendulum, so that the voltage generated in the coil can be used for the feedback. This voltage is amplified and then fed to the driving coil through a variable resistor. In our setup, the amplifier is PASCO's *Digital function generator–amplifier* (PI-9587C), and the variable resistor is PASCO's *Decade resistance box* (PI-9588). The pulses of electric current are supplied to the driving coil every time the angular velocity of the pendulum reaches a maximum (figure 5). The sign of the feedback depends on the polarity of the two coils.

The motion equation for the pendulum with positive or negative feedback can be presented in a form similar to the Van der Pol equation (e.g., Moon (1987)):

$$\theta'' + [\gamma \pm \beta(\theta)]\theta' + \omega_0^2\theta = 0, \tag{3}$$

where β is the feedback coefficient, which depends on the angular position. The plus sign is taken for negative feedback, and minus for positive.

The free oscillations of the pendulum are recorded for different values of the feedback factor controllable by the variable resistor. The decay constant is determined by graphing the function $A\exp(-Bt)$, as described above. The feedback factor is proportional to the current in the driving coil, that is, inversely proportional to the full resistance of the feedback circuit including the coil. The inverse resistance is therefore taken as a measure of the feedback factor. The decay constant is a linear function of the feedback factor. In these measurements, the gap between the upper magnet and the magnetic core of the driving coil is 40 mm, and moderate magnetic damping is used to make the decay exponential.

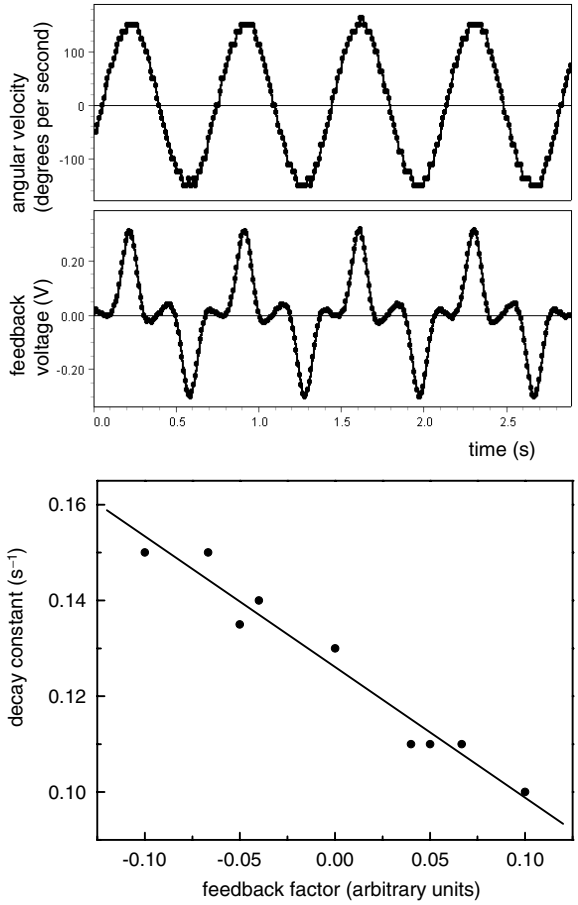

Figure 5. From top to bottom: angular velocity, voltage across the feedback coil, and the decay constant of the pendulum versus the feedback factor.

4. Forced oscillations

For observing forced oscillations, the driving coil is connected to the PASCO's *Power amplifier II* (CI-6552A) governed by the *Signal generator* incorporated into the *ScienceWorkshop 750 Interface*. The amplifier provides currents of ultra-low frequency, so that the upper magnet aligned horizontally is subjected to a magnetic field directed in turn down and up. The interaction of the magnet with the field produces a periodic driving torque. The experiments relate to several topics: the tuning curves including hysteresis and amplitude and phase jumps, regular nonlinear oscillations, and chaotic motion. The transient processes after changing the amplitude or frequency of the driving torque or the response to a step or an impulse function are observable as well.

4.1. Tuning curves

When determining the tuning curves of the pendulum, the oscillations only slightly differ from harmonic ones due to reduced driving currents. Therefore, they can be approximated by a sinusoid. *DataStudio* stores data on the current passing through the driving coil and the

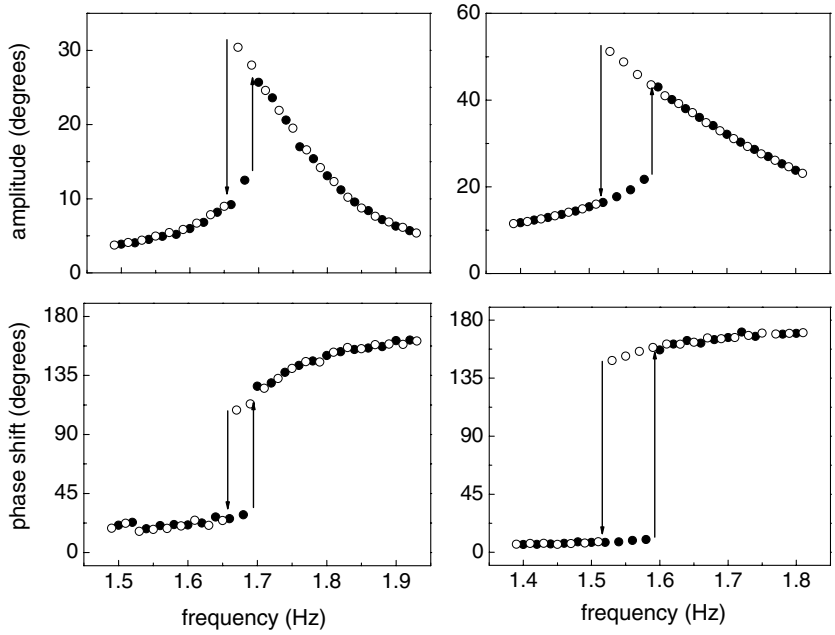

Figure 6. Example of tuning curves for 0.05 A (left) and 0.2 A (right) amplitudes of driving current: ●—increasing frequency, ○—decreasing frequency.

angular position of the pendulum. The *Fit/Sine fit* tool fits both data by equation (2). From the two fits, one immediately obtains the amplitude of the oscillations and the phase shift between the driving torque and the angular position of the pendulum. The phase shift between the two quantities equals $\Delta\varphi = 2\pi(C_1 - C_2)/B$, where C_1 and C_2 are the quantities in the two fits. It is useful to check beforehand that at low frequencies the driving torque and the angular position of the pendulum are in phase; otherwise, it is necessary to alter the polarity of the current feeding the driving coil.

In the measurements (see figure 2(c)), the gap between the upper magnet and the driving coil is 40 mm, and moderate magnetic damping is used. The nonlinearity is brought in by the 320-turn coil providing attractive action on the lower magnet. The dc current in this coil is 0.5 A. The data obtained are similar to those usually observable under such conditions (Dixon *et al* (1985), Grosu and Ursu (1986), Peters (1996)). An advantage of *DataStudio* is the possibility of determining, along with the oscillation amplitudes, the phase shifts between the driving torque and the oscillation of the pendulum (figure 6). Due to the additional nonlinearity, the hysteresis and the amplitude and phase jumps in the vicinity of resonance are seen even for small-angle oscillations.

With the data-acquisition system, it is possible to record the transients after changing the amplitude or frequency of the driving torque. In the vicinity of resonance, the nonlinear oscillations become very sensitive to such changes.

4.2. Regular nonlinear oscillations

In these experiments (see figure 2(d)), the gap between the magnetic core of the driving coil and the upper magnet is 20 mm. *DataStudio* displays the oscillations as time series and phase plane plots, so that the nonlinear behaviour of the pendulum is clearly seen. The frequency and

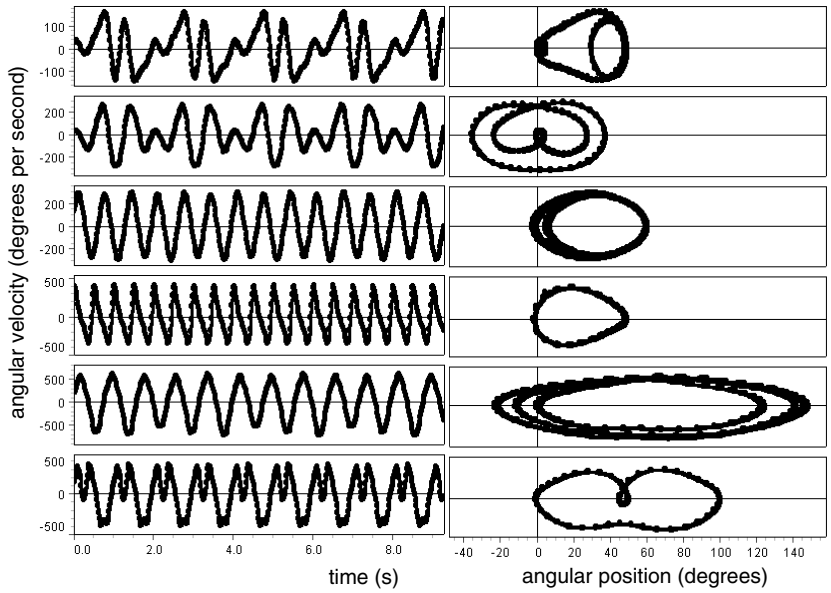

Figure 7. Time series of angular velocity and phase plane plots for different frequencies and amplitudes of driving current. From top to bottom: 0.5 Hz, 0.2 A; 1 Hz, 0.1 A; 1.5 Hz, 0.2 A; 2 Hz, 0.8 A; 2.5 Hz, 0.4 A; 3 Hz, 0.45 A.

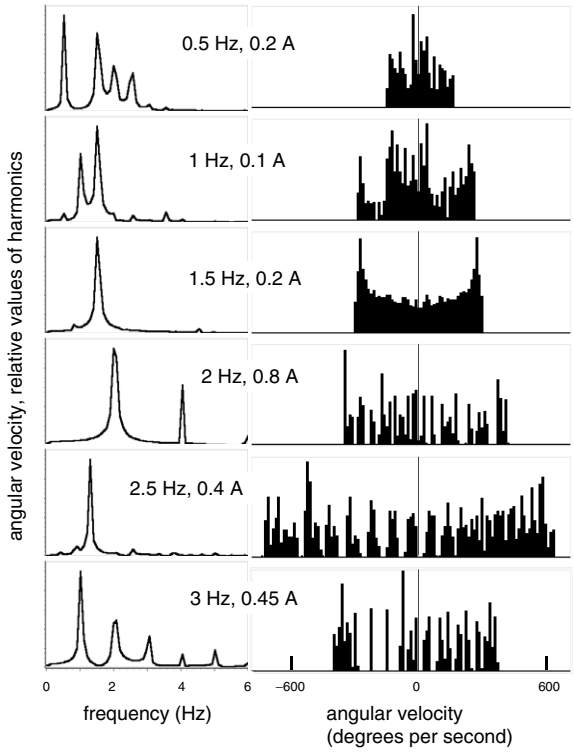

Figure 8. Fourier spectra and histograms of angular velocity for the examples shown in figure 7.

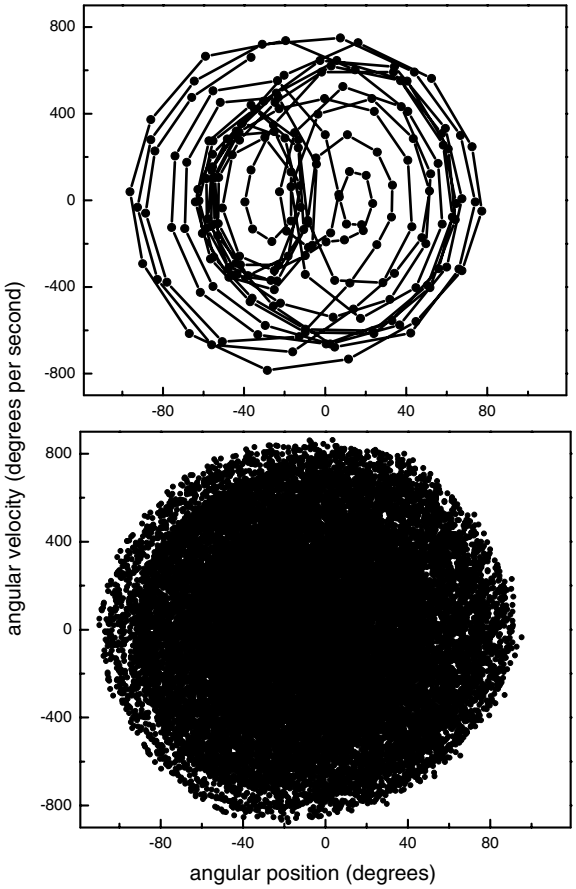

Figure 9. Phase plane plots for the initial part of chaotic motion (10 s, 200 points) and for the whole run (1500 s, 30 000 points).

amplitude of the drive current are set via the dialogue box of the *Signal generator*. Records of the oscillations are taken when steady oscillations are well established. The PASCO's *Rotary motion sensor* measures the displacement of the pendulum from the point where the experimenter starts the measurement or when the angular position or velocity of the pendulum reaches a value preset by the experimenter. In many cases, records of the angular velocity are advantageous.

Examples shown here represent various nonlinear oscillations, including harmonic and subharmonic generation (figure 7). The appearance of subharmonics is one of possible routes to chaos. In addition, the *Fast Fourier transform* tool of *DataStudio* shows Fourier spectra of the angular position or velocity, and the *Histogram* tool displays their probability distributions (figure 8). The results presented are obtained with no magnetic damping and modifications of the restoring torque by the lower coil.

4.3. Chaotic motion

With high driving torques, chaotic motion of the pendulum is attainable. In these measurements, the gap between the magnetic core of the driving coil and the upper magnet is reduced to 15 mm. The amplitude of the drive current is 0.8 A.

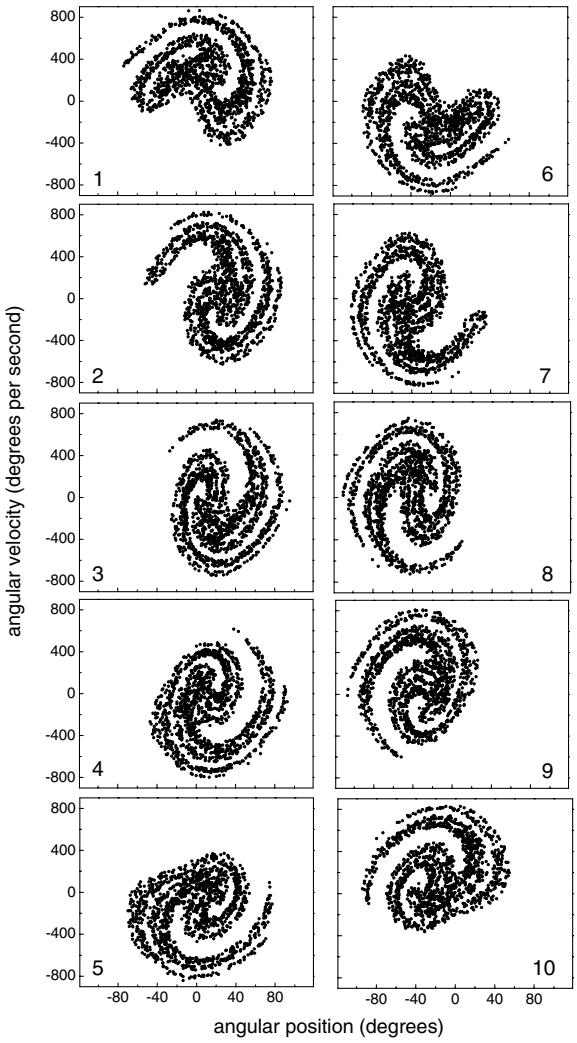

Figure 10. Poincaré maps for chaotic motion taken at phases separated by 1/10 of the period (1500 points each).

It is a common practice to characterize chaotic motion with the so-called Poincaré sections (Poincaré maps). *DataStudio* employs the same clock for generating the drive current and for sampling the measurement data. Therefore, data for the Poincaré maps can be unmistakably stored during unlimited time. In our measurements, the period of the driving torque is 1 s, so that the Poincaré maps could be taken with a 1 Hz sample rate. However, in this case *DataStudio* calculates the angular position and velocity as averages for 1 s intervals, which are not representative. We use a 20 Hz sample rate, so that the quantities to be measured are averages for a 1/20 part of the period. With this sample rate, 20 data points are stored during each period of the driving torque, and 20 Poincaré maps at particular phases of the period become available in one run. In a run lasting 1500 s, *DataStudio* stores 30 000 data points for the angular position and velocity of the pendulum. The phase plane plots for the initial 10 s and for the whole run are shown here (figure 9).

To extract necessary data to plot all the Poincaré maps, a simple software for *Microsoft Excel* was prepared. This easy task may be opened for student activities; therefore, the software is not given here. The program gathers data points numbered $1, 21, 41, \ldots$ (1500 points in total) and plots the corresponding Poincaré map. The same operation is simultaneously performed for data points numbered $2, 22, 42, \ldots$ and so on. Twenty Poincaré maps for phases separated by $1/20$ part of the period of the driving torque are thus obtainable from the data stored by *DataStudio*.

For obtaining sharp Poincaré maps for chaotic motion, the pendulum should be highly damped (Moon (1987), DeSerio (2003)). In our case, the damping is provided by a permanent magnet positioned close to the surface of the aluminium disc attached to the axle of the *Rotary motion sensor*. Ten Poincaré maps for phases separated by $1/10$ part of the period of the driving torque are presented here (figure 10). Note the symmetry in the maps separated by 180° (maps numbered 1 and 6, 2 and 7, and so on). For obtaining Poincaré maps for definite phases of the drive torque, we use the *Auto* mode of the *Signal generator*. In this mode, the generator starts to produce the driving current at the same instant as the measurements are triggered. To eliminate data stored during the transient process, it is enough to remove data for the first 10 s of the run (the first 200 data points). With this procedure, the software builds the Poincaré maps every time for the same phases of the driving torque.

It is possible to confirm that the Poincaré maps depend on the decay of the pendulum. DeSerio (2003) presented a very convincing experimental proof of this statement. In our case, the decay constant cannot be changed in a wide range because of the damping action of the driving coil.

The results obtained show that the low-cost magnetically controlled pendulum is quite suitable for observing chaotic motion.

5. Conclusions

The setups described are extremely simple and can be assembled in a short time. Despite its simplicity, the apparatus provides many options for studying oscillations of a pendulum, including nonlinear oscillations and chaotic motion. The apparatus offers many options for further experimentation, including varying the natural frequency of the oscillator, the decay constant, and the strength of nonlinearity. Due to the possibilities of modifying the parameters of the pendulum, the experiments are very suitable for student projects. They could include topics of different levels: large-angle oscillations of a pendulum; a pendulum with additional nonlinearity; forced oscillations of a pendulum subjected to repulsive or attractive action of a dc magnetic field; Poincaré maps for different decay of the pendulum, and so on.

Acknowledgment

I am grateful to my son Alex for preparing the software used here for displaying the Poincaré maps.

References

Baker G L 2006 Probability, pendulums, and pedagogy *Am. J. Phys.* **74** 482–9
Baker G L and Gollub J P 1996 *Chaotic Dynamics: An Introduction* 2nd edn (Cambridge: Cambridge University Press)
Berdahl J P and Vander Lugt K 2001 Magnetically driven chaotic pendulum *Am. J. Phys.* **69** 1016–9
Blackburn J A and Baker G L 1998 A comparison of commercial chaotic pendulums *Am. J. Phys.* **66** 821–30
DeSerio R 2003 Chaotic pendulum: the complete attractor *Am. J. Phys.* **71** 250–7

Dixon M, Lowell J and Lyon S 1985 Amplitude jumps of a nonlinear oscillator *Eur. J. Phys.* **6** 72–9
Grosu I and Ursu D 1986 Linear and nonlinear oscillations: an experiment for students *Eur. J. Phys.* **7** 91–4
José J V and Saletan E J 1998 *Classical Dynamics: A Contemporary Approach* (Cambridge: Cambridge University Press)
Kautz R L 1993 Chaos in a computer-animated pendulum *Am. J. Phys.* **61** 407–15
Kraftmakher Y 2005 Computerized physical pendulum for classroom demonstrations *Phys. Teach.* **43** 244–6
Kraftmakher Y 2007a *Experiments and Demonstrations in Physics. Bar-Ilan Physics Laboratory* (Singapore: World Scientific)
Kraftmakher Y 2007b Magnetic field of a dipole and the dipole–dipole interaction *Eur. J. Phys.* **28** 409–14
Laws P W 2004 A unit on oscillations, determinism and chaos for introductory physics students *Am. J. Phys.* **72** 446–52
Lewowski T and Woźniak K 2002 The period of a pendulum at large amplitudes: a laboratory experiment *Eur. J. Phys.* **23** 461–4
Marega E, Zilio S C and Ioriatti L 1990 Electromechanical analog for Landau's theory of second-order symmetry-breaking transitions *Am. J. Phys.* **58** 655–9
Moon F C 1987 *Chaotic Vibrations* (New York: Wiley)
Peters R D 1996 Resonance response of a moderately driven rigid planar pendulum *Am. J. Phys.* **60** 170–3
Pippard A B 1978 *The Physics of Vibration* (Cambridge: Cambridge University Press)
Schmidt V H and Childers B R 1984 Magnetic pendulum apparatus for analog demonstration of first-order and second-order phase transitions and tricritical points *Am. J. Phys.* **52** 39–43
Siahmakoun A, French V A and Patterson J 1997 Nonlinear dynamics of a sinusoidally driven pendulum in a repulsive magnetic field *Am. J. Phys.* **65** 393–400
Squire P T 1986 Pendulum damping *Am. J. Phys.* **54** 984–91
Thornton S T and Marion J B 2004 *Classical Dynamics of Particles and Systems* 5th edn (Belmont, CA: Brooks/Cole)